# ANALYSIS OF SHELL STRUCTURES BY A CELL-BASED SMOOTHED DISCRETE SHEAR GAP METHOD USING TRIANGULAR ELEMENTS

**Nguyen Thoi Trung[1,2], Phung Van Phuc[1], Luong Van Hai[3], Thai Hoang Chien[1] and Nguyen Xuan Hung[1,2]**

## ABSTRACT

**The cell-based strain smoothing technique is combined with the discrete shear gap method (DSG3) using three-node triangular elements to give a so-called cell-based smoothed discrete shear gap method (CS-DSG3) for static and free vibration analyses of Reissner-Mindlin shells. In the process of formulating the system stiffness matrix of the CS-DSG3, each triangular element will be divided into three sub-triangles, and in each sub-triangle, the stabilized DSG3 is used to compute the strains and to avoid the transverse shear locking. Then the strain smoothing technique on whole the triangular element is used to smooth the strains on these three sub-triangles. The CS-DSG3 hence not only overcomes the drawback of the DSG3 which depends on the sequence of node numbers of elements, but also improve the accuracy as well as the stability of the DSG3. The numerical examples demonstrated that the CS-DSG3 is free of shear locking and achieves the high accuracy compared to others existing shell elements.**

Key words: *Reissner-Mindlin shell, Shear locking, Cell-based smoothed discrete shear gap technique (CS-DSG3), Smoothed finite element method, Strain smoothing technique*

## 1. INTRODUCTION

The numerical analysis of shell structures in large-scale industrial problems has always been a challenge and receives continuously strong interest [1]. In the past three decades, the finite element method (FEM) has been used as a powerful numerical tool to simulate behaviors of shell structures [2]. Compared with four-node quadrilateral shell elements [3,4], three-node triangular shell elements [5,6] is particular attractive due to its simplicity, automatic meshing and re-meshing in adaptive analysis. However, the derivation of simple and effective three-node triangular shell elements for analysis of general shell structures with complex loading and boundary conditions is still a challenging research topic. This paper hence focuses on developing such a simple and effective three-node triangular shell element.

Recently, Bletzinger et al. [9] proposed a three-node triangular shell element DSG3 based on the Discrete Shear Gap method (DSG) which can be classified as an assumed natural strains (ANS) element [7]. In the DSG3, the shear strain is linear interpolated from the shear gaps of displacement along the sides of the elements by using the standard element shape functions. The DSG3 shell element can satisfy explicitly the kinematic equation for the shear strains at discrete points and effectively eliminates the parasitic shear strains. However, the element stiffness matrix in the DSG3 still depends on the sequence of node numbers, and hence the solution of DSG3 is influenced when the sequence of node numbers changes, especially for the coarse and distorted meshes.

In addition, the overly stiff behavior is usually observed in many Reissner-Mindlin shell elements based on compatible displacement-based FEM models. The overly stiff behavior is even more severe when three-node triangular shell elements are used. In order to reduce the overly stiffness of the displacement-based FEM models, Liu and Nguyen-Thoi et al. [10-12] proposed a cell-based smoothed finite element method (CS-FEM) which is a combination of the standard FEM and a strain smoothing technique [13] used in meshfree methods. In the CS-FEM, the domain discretization is still based on elements as in the FEM, however the stiffness matrices are calculated based over smoothing domains located inside the elements. The CS-FEM, however so far, has been developed mainly only for the 4-node quadrilateral elements [10-12] and the improvement of accuracy of solutions compared to those of FEM is still marginal.

This paper hence extends the CS-FEM for triangular elements and for significant improvement of solutions of shell analysis. The cell-based strain smoothing technique in the CS-FEM is combined with the DSG3 [9] using three-node triangular elements to give a so-called the cell-based smoothed discrete shear gap method (CS-DSG3) for static and free vibration analyses of Reissner-Mindlin shells. In the process of formulating the system stiffness matrix of the CS-DSG3, each triangular element will be divided into three sub-triangles, and in each sub-triangle the stabilized DSG3 [14] is used to compute the strains and to avoid the transverse shear locking. Then the strain smoothing technique on whole the triangular element is used to

smooth the strains on these three sub-triangles. The CS-DSG3 hence not only overcomes the drawback of the DSG3 which depends on the sequence of node numbers of elements, but also improve the accuracy as well as the stability of the DSG3.

## 2. WEAKFORM AND GENERAL FEM FORMULATION FOR THE REISSNER-MINDLIN SHELL

### 2.1. Weak Form for the Reissner-Mindlin Shell

Consider a shell subjected to both membrane forces and bending forces. The middle (neutral) surface of shell is chosen as the reference plane that occupies a domain $\Omega \in \mathbb{R}^3$ as shown in Figure 1. Let u, v, w be the displacements of the middle plane in the x, y, z directions, and $\beta_x$, $\beta_y$, $\beta_z$ are the rotations of the middle plane around y-axis, x–axis, and z–axis respectively, with the positive directions defined as shown in Figure 1.

The unknown vector of six independent field variables at any point in the problem domain of the Reissner-Mindlin shells can be written as $\mathbf{u} = \begin{bmatrix} u & v & w & \beta_x & \beta_y & \beta_z \end{bmatrix}$. The membrane strain $\boldsymbol{\varepsilon}^m$, the curvature of deflected shell $\boldsymbol{\kappa}$ and the shear strains $\boldsymbol{\gamma}$ are defined, respectively, as

$$\left(\boldsymbol{\varepsilon}^m\right)^T = \begin{bmatrix} \frac{\partial u}{\partial x} & \frac{\partial v}{\partial y} & \frac{\partial u}{\partial y} + \frac{\partial v}{\partial x} \end{bmatrix}$$

$$\boldsymbol{\kappa}^T = \begin{bmatrix} \frac{\partial \beta_x}{\partial x} & \frac{\partial \beta_y}{\partial y} & \frac{\partial \beta_x}{\partial y} + \frac{\partial \beta_y}{\partial x} \end{bmatrix}$$

$$\boldsymbol{\gamma} = \begin{bmatrix} \frac{\partial w}{\partial x} + \beta_x \\ \frac{\partial w}{\partial y} + \beta_y \end{bmatrix} \qquad (1)$$

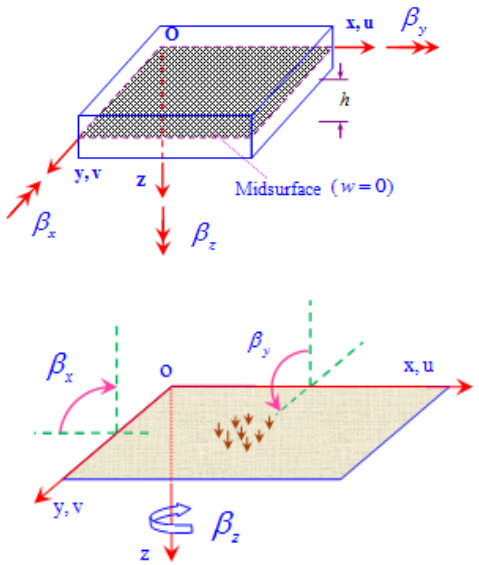


Figure 1: Reissner-Mindlin thick shell and positive directions of the displacement w and two rotations $\beta_x$, $\beta_y$, $\beta_z$

The standard Galerkin weakform of the static equilibrium equations for the Reissner-Mindlin shell can now be written as [1]:

$$\int_\Omega \left(\delta\boldsymbol{\varepsilon}^m\right)^T \mathbf{D}^m\boldsymbol{\varepsilon}^m \, d\Omega + \int_\Omega \delta\boldsymbol{\kappa}^T \mathbf{D}^b\boldsymbol{\kappa} \, d\Omega + \int_\Omega \delta\boldsymbol{\gamma}^T \mathbf{D}^s\boldsymbol{\gamma} \, d\Omega = \int_\Omega \delta\mathbf{u}^T\mathbf{b} \, d\Omega \qquad (2)$$

where $\mathbf{b} = \begin{bmatrix} 0 & 0 & p(x,y,z) & 0 & 0 & 0 \end{bmatrix}^T$ is the distributed load. The matrices $\mathbf{D}^m$, $\mathbf{D}^b$ and $\mathbf{D}^s$ are the material matrices related to the membrane, bending and shear deformation, respectively.

For the free vibration analysis of Reissner-Mindlin shells, the standard Galerkin weakform can be derived from the dynamic form of energy principle [1]:

$$\int_\Omega \left(\delta\boldsymbol{\varepsilon}^m\right)^T \mathbf{D}^m\boldsymbol{\varepsilon}^m \, d\Omega + \int_\Omega \delta\boldsymbol{\kappa}^T \mathbf{D}^b\boldsymbol{\kappa} \, d\Omega + \int_\Omega \delta\boldsymbol{\gamma}^T \mathbf{D}^s\boldsymbol{\gamma} \, d\Omega + \int_\Omega \delta\mathbf{u}^T\mathbf{m}\ddot{\mathbf{u}} \, d\Omega = 0$$

where m is the matrix containing the mass density of the material $\rho$ and thickness $t$.

### 2.2. General FEM Formulation for Reissner-Mindlin Flat Shell Elements

Now, discretize the bounded domain $\Omega$ into $N_e$ finite elements such that $\Omega = \bigcup_{e=1}^{N_e} \Omega_e$ and $\Omega_i \cap \Omega_j \neq \varnothing, i \neq j$, then the finite element solution $\mathbf{u}^h = \begin{bmatrix} u & v & w & \beta_x & \beta_y & \beta_z \end{bmatrix}^T$ of a displacement model for the Reissner-Mindlin shell is expressed as:

$$\mathbf{u}^h = \sum_{I=1}^{N_n} \mathbf{N}_I\mathbf{d}_I \qquad (4)$$

where $N_n$ is the total number of nodes of problem domain discretized, $\mathbf{N}_I(\mathbf{x})$ is the shape function matrix at node $I$, $\mathbf{d}_I = \begin{bmatrix} u_I & v_I & w_I & \beta_{xI} & \beta_{yI} & \beta_{zI} \end{bmatrix}^T$ is the displacement vector of the nodal degrees of freedom of $\mathbf{u}^h$ associated to node I, respectively.

The membrane, bending and shear strains can be then expressed in the matrix forms as:

$$\boldsymbol{\varepsilon}^m = \sum_I \mathbf{R}_I\mathbf{d}_I \quad , \quad \boldsymbol{\kappa} = \sum_I \mathbf{B}_I\mathbf{d}_I \quad , \quad \boldsymbol{\gamma}^s = \sum_I \mathbf{S}_I\mathbf{d}_I \qquad (5)$$

where $\mathbf{R}_I$, $\mathbf{B}_I$ and $\mathbf{S}_I$ are the matrices containing the derivatives of the shape functions.

The discretized system of equations of the Reissner-Mindlin shell using the FEM for static analysis then can be expressed as,

$$\mathbf{K}\mathbf{d} = \mathbf{F} \qquad (6)$$

where $\mathbf{K}$ is the global stiffness matrix given by

$$\mathbf{K} = \int_\Omega \mathbf{R}^T\mathbf{D}^m\mathbf{R} \, d\Omega + \int_\Omega \mathbf{B}^T\mathbf{D}^b\mathbf{B} \, d\Omega + \int_\Omega \mathbf{S}^T\mathbf{D}^s\mathbf{S} \, d\Omega \qquad (7)$$

and $\mathbf{F}$ is the load vector defined as

$$\mathbf{F} = \int_\Omega p\mathbf{N} \, d\Omega + \mathbf{f}^b \qquad (8)$$

in which $\mathbf{f}^b$ is the remaining part of $\mathbf{F}$ subjected to prescribed boundary loads.

For free vibration analysis, we have

$$(\mathbf{K} - \omega^2\mathbf{M})\mathbf{d} = \mathbf{0} \qquad (9)$$

where $\omega$ is the natural frequency and $\mathbf{M}$ is the global mass matrix defined by

$$\mathbf{M} = \int_{\Omega} \mathbf{N}^T \mathbf{m} \mathbf{N}^T \mathrm{d}\Omega \tag{10}$$

## 3. FEM FORMULATION OF THE THREE-NODE TRIANGULAR FLAT SHELL ELEMENT CS-DSG3

### 3.1. Brief on the DSG3 Formulation

The formulation of the stabilized DSG3 [9] is based on the concept "shear gap" of displacement along the sides of the elements. The DSG3 element is shear-locking-free and has several superior properties as presented in Ref [9]. In this paper, we just brief on the DSG3 formulation which is necessary for the formulation of the CS-DSG3.

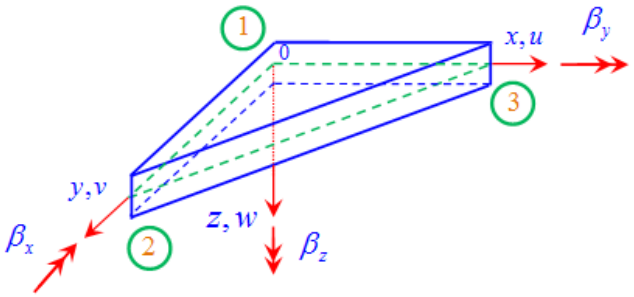


Figure 2: Three-node triangular element

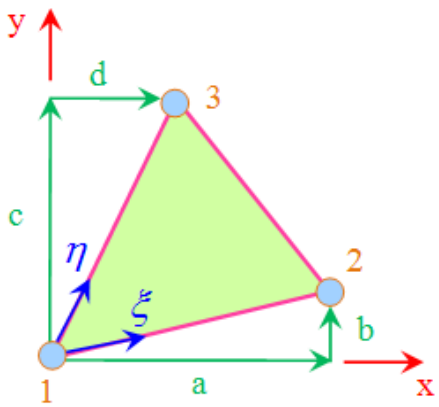


Figure 3: Three-node triangular element and local coordinates in the DSG3

Using a mesh of triangular elements, the approximation $\mathbf{u}^h$ for a 3-node triangular element $\Omega_e$ shown in Figure 2 for the Reissner-Mindlin shell can be written, at the element level, as

$$\mathbf{u}_e^h = \sum_{I=1}^{3} \mathbf{N}_I \mathbf{d}_I \tag{11}$$

where $\mathbf{d}_{eI} = \begin{bmatrix} u_I & v_I & w_I & \beta_{xI} & \beta_{yI} & \beta_{zI} \end{bmatrix}^T$ are the nodal degrees of freedom of $\mathbf{u}_e^h$ associated to node I and $\mathbf{N}_I(\mathbf{x})$ are the matrices of linear shape functions in a natural coordinate defined by

$$N_1 = 1 - \xi - \eta, \quad N_2 = \xi, \quad N_3 = \eta \tag{12}$$

The membrane strain and curvatures of the deflection in the element are then obtained by

$$\boldsymbol{\varepsilon}^{mh} = \underbrace{\begin{bmatrix} \mathbf{R}_1 & \mathbf{R}_2 & \mathbf{R}_3 \end{bmatrix}}_{\mathbf{R}} \mathbf{d}_e = \mathbf{R}\mathbf{d}_e \ ;$$

$$\boldsymbol{\kappa}^h = \underbrace{\begin{bmatrix} \mathbf{B}_1 & \mathbf{B}_2 & \mathbf{B}_3 \end{bmatrix}}_{\mathbf{B}} \mathbf{d}_e = \mathbf{B}\mathbf{d}_e \tag{13}$$

where $\mathbf{d}_e = \begin{bmatrix} \mathbf{d}_{e1} & \mathbf{d}_{e2} & \mathbf{d}_{e3} \end{bmatrix}^T$ is the nodal displacement vector of element, $\mathbf{R}$ and $\mathbf{B}$ contains the derivatives of the shape functions that are constants in which

$$\mathbf{R}_1 = \begin{bmatrix} b-c & 0 & 0 & 0 & 0 & 0 \\ 0 & d-a & 0 & 0 & 0 & 0 \\ d-a & b-c & 0 & 0 & 0 & 0 \end{bmatrix};$$

$$\mathbf{R}_2 = \begin{bmatrix} c & 0 & 0 & 0 & 0 & 0 \\ 0 & -d & 0 & 0 & 0 & 0 \\ -d & c & 0 & 0 & 0 & 0 \end{bmatrix};$$

$$\mathbf{R}_3 = \begin{bmatrix} -b & 0 & 0 & 0 & 0 & 0 \\ 0 & a & 0 & 0 & 0 & 0 \\ a & -b & 0 & 0 & 0 & 0 \end{bmatrix} \tag{14}$$

$$\mathbf{B}_1 = \begin{bmatrix} 0 & 0 & 0 & b-c & 0 & 0 \\ 0 & 0 & 0 & 0 & d-a & 0 \\ 0 & 0 & 0 & d-a & b-c & 0 \end{bmatrix};$$

$$\mathbf{B}_2 = \begin{bmatrix} 0 & 0 & 0 & c & 0 & 0 \\ 0 & 0 & 0 & 0 & -d & 0 \\ 0 & 0 & 0 & -d & c & 0 \end{bmatrix};$$

$$\mathbf{B}_3 = \begin{bmatrix} 0 & 0 & 0 & -b & 0 & 0 \\ 0 & 0 & 0 & 0 & a & 0 \\ 0 & 0 & 0 & a & -b & 0 \end{bmatrix} \tag{15}$$

with $a = x_2 - x_1, b = y_2 - y_1, c = y_3 - y_1, d = x_3 - x_1$ as shown in Figure 3, and $\mathbf{x}_i = \begin{bmatrix} x_i & y_i \end{bmatrix}^T$, $i = 1,2,3$, are coordinates of three nodes in the local coordinate system, respectively and $A_e$ is the area of the triangular element.

In order to overcome the shear locking, Bletzinger et al. [9] proposed the discrete shear gap method (DSG3) to alter the shear strain field. The altered shear strains are in the form of

$$\boldsymbol{\gamma}^h = \underbrace{\begin{bmatrix} \mathbf{S}_1 & \mathbf{S}_2 & \mathbf{S}_3 \end{bmatrix}}_{\mathbf{S}} \mathbf{d}_e = \mathbf{S}\mathbf{d}_e \tag{16}$$

where

$$\mathbf{S}_1 = \frac{1}{2A_e} \begin{bmatrix} 0 & 0 & b-c & A_e & 0 & 0 \\ 0 & 0 & d-a & 0 & A_e & 0 \end{bmatrix} \tag{17}$$

$$\mathbf{S}_2 = \frac{1}{2A_e} \begin{bmatrix} 0 & 0 & c & ac/2 & bc/2 & 0 \\ 0 & 0 & -d & -ad/2 & -bd/2 & 0 \end{bmatrix} \tag{18}$$

$$\mathbf{S}_3 = \frac{1}{2A_e} \begin{bmatrix} 0 & 0 & -b & -bd/2 & -bc/2 & 0 \\ 0 & 0 & a & ad/2 & ac/2 & 0 \end{bmatrix} \tag{19}$$

Substituting matrices $\mathbf{R}$, $\mathbf{B}$, and $\mathbf{S}$ in Eqs. (13) and (16)

into Eq. (7), the global stiffness matrix now becomes

$$\mathbf{K}^{\mathrm{DSG3}} = \sum_{e=1}^{N_e} \mathbf{K}_e^{\mathrm{DSG3}} \qquad (20)$$

where $\mathbf{K}_e^{\mathrm{DSG3}}$ is the element stiffness matrix of the DSG3 element and is given by

$$\begin{aligned}\mathbf{K}_e^{\mathrm{DSG3}} &= \mathbf{T}^T\left(\int_{\Omega_e}\mathbf{R}^T\mathbf{D}^m\mathbf{R}\,\mathrm{d}\Omega + \int_{\Omega_e}\mathbf{B}^T\mathbf{D}^b\mathbf{B}\,\mathrm{d}\Omega + \int_{\Omega_e}\mathbf{S}^T\mathbf{D}^s\mathbf{S}\,\mathrm{d}\Omega\right)\mathbf{T} \\ &= \mathbf{T}^T\underbrace{\left(\mathbf{R}^T\mathbf{D}^m\mathbf{R}\,A_e + \mathbf{B}^T\mathbf{D}^b\mathbf{B}\,A_e + \mathbf{S}^T\mathbf{D}^s\mathbf{S}\,A_e\right)}_{\mathbf{k}_e}\mathbf{T} = \mathbf{T}^T\mathbf{k}_e\mathbf{T}\end{aligned} \qquad (21)$$

in which $\mathbf{k}_e$ is the element stiffness matrix computed in the local coordinate system $\hat{x}\hat{y}\hat{z}$, and $\mathbf{T}$ is the transformation matrix of coordinates from the global coordinate system $xyz$ to the local coordinate system $\hat{x}\hat{y}\hat{z}$.

It was suggested [14] that a stabilization term needs to be added to the original DSG3 element to further improve the accuracy of approximate solutions and to stabilize shear force oscillations. Such a modification is achieved by simply replacing $\mathbf{D}^s$ in Eq. (21) by $\hat{\mathbf{D}}^s$, as follows.

$$\mathbf{K}_e^{\mathrm{DSG3}} = \mathbf{T}^T\underbrace{\left(\mathbf{R}^T\mathbf{D}^m\mathbf{R}\,A_e + \mathbf{B}^T\mathbf{D}^b\mathbf{B}\,A_e + \mathbf{S}^T\hat{\mathbf{D}}^s\mathbf{S}\,A_e\right)}_{\mathbf{k}_e}\mathbf{T} = \mathbf{T}^T\mathbf{k}_e\mathbf{T} \qquad (22)$$

where

$$\hat{\mathbf{D}}^s = \frac{kt^3}{t^2+\alpha h_e^2}\begin{bmatrix}1 & 0\\ 0 & 1\end{bmatrix} \qquad (23)$$

in which $h_e$ is the longest length of the edges of the element and $\alpha$ is a positive constant [15].

From Eqs. (13), (16) and (22), it is clear that the values of element stiffness matrix at the drilling degree of freedom $\beta_z$ equal zero which can cause the singularity in the global stiffness matrix when all the elements meeting at a node are coplanar. To deal with this issue, the null values of the stiffness corresponding to the drilling degree of freedom are then replaced by approximate values. This approximate value is taken to be equal to 10-3 times the maximum diagonal value in the element stiffness matrix [8].

Also from Eqs. (13), (16) and (22), it is clearly seen that the element stiffness matrix in the DSG3 depends on the sequence of node numbers of elements, and hence the solution of DSG3 is influenced when the sequence of node numbers of elements changes, especially for the coarse and distorted meshes. The CS-DSG3 is hence proposed to overcome this drawback and also improve the accuracy as well as the stability of the DSG3.

### 3.2. Formulation of CS- DSG3

Consider a typical triangular element $\Omega_e$ as shown in Figure 4. We first divide the element into three sub-triangles $\Delta_1$, $\Delta_2$ and $\Delta_3$ such as $\Omega_e = \bigcup_{i=1}^{3}\Delta_i$ and $\Delta_i \cap \Delta_j = \varnothing, i \neq j$, by simply connecting the central point $O$ of the triangle with 3 field nodes as shown in Figure 4.

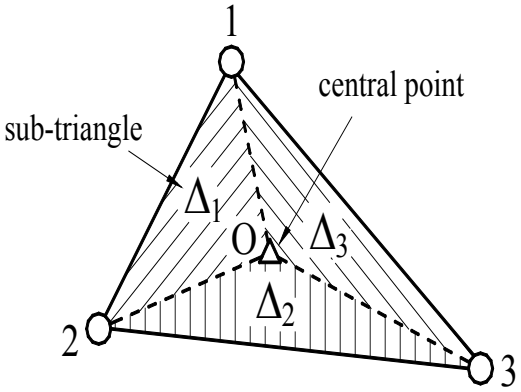


Figure 4: Three sub-triangles ($\Delta_1$, $\Delta_2$ and $\Delta_3$) created from the triangle 1-2-3 in the CS-DSG3 by connecting the central point $O$ with three field nodes 1, 2 and 3

In the CS-DSG3, we assume that the displacement vector $\mathbf{d}_{eO}$ at the central point $O$ is the simple average of three displacement vectors $\mathbf{d}_{e1}$, $\mathbf{d}_{e2}$ and $\mathbf{d}_{e3}$ of three field nodes

$$\mathbf{d}_{eO} = \frac{1}{3}\left(\mathbf{d}_{e1} + \mathbf{d}_{e2} + \mathbf{d}_{e3}\right) \qquad (24)$$

On the first sub-triangle $\Delta_1$, we now construct a linear approximation $\mathbf{u}_e^{\Delta_1} = \begin{bmatrix}u_e & v_e & w_e & \beta_{ex} & \beta_{ey} & \beta_{ez}\end{bmatrix}^T$ by

$$\mathbf{u}_e^{\Delta_1} = N_1^{\Delta_1}(\mathbf{x})\mathbf{d}_{eO} + N_2^{\Delta_1}(\mathbf{x})\mathbf{d}_{e1} + N_3^{\Delta_1}(\mathbf{x})\mathbf{d}_{e2} = \left(\mathbf{N}^{\Delta_1}(\mathbf{x})\right)^T\mathbf{d}^{\Delta_1} \qquad (25)$$

where $\mathbf{d}^{\Delta_1} = \begin{bmatrix}\mathbf{d}_{eO} & \mathbf{d}_{e1} & \mathbf{d}_{e2}\end{bmatrix}^T$ is the vector of nodal degrees of freedom of sub-triangle $\Delta_1$ and $\mathbf{N}^{\Delta_1} = \begin{bmatrix}N_1^{\Delta_1} & N_2^{\Delta_1} & N_3^{\Delta_1}\end{bmatrix}^T$ is vector of shape functions in a natural coordinate defined by Eq. (12).

The membrane strain $\boldsymbol{\varepsilon}^{m\Delta_1}$, the curvatures of the deflection $\boldsymbol{\kappa}^{\Delta_1}$ and the altered shear strains $\boldsymbol{\gamma}^{\Delta_1}$ in the sub-triangle $\Delta_1$ are then obtained by

$$\boldsymbol{\varepsilon}^{m\Delta_1} = \underbrace{\begin{bmatrix}\mathbf{r}_1^{\Delta_1} & \mathbf{r}_2^{\Delta_1} & \mathbf{r}_3^{\Delta_1}\end{bmatrix}}_{\mathbf{r}^{\Delta_1}}\begin{bmatrix}\mathbf{d}_{eO}\\ \mathbf{d}_{e1}\\ \mathbf{d}_{e2}\end{bmatrix} = \mathbf{r}^{\Delta_1}\mathbf{d}^{\Delta_1} \qquad (26)$$

$$\boldsymbol{\kappa}^{\Delta_1} = \underbrace{\begin{bmatrix}\mathbf{b}_1^{\Delta_1} & \mathbf{b}_2^{\Delta_1} & \mathbf{b}_3^{\Delta_1}\end{bmatrix}}_{\mathbf{b}^{\Delta_1}}\begin{bmatrix}\mathbf{d}_{eO}\\ \mathbf{d}_{e1}\\ \mathbf{d}_{e2}\end{bmatrix} = \mathbf{b}^{\Delta_1}\mathbf{d}^{\Delta_1} \qquad (27)$$

$$\boldsymbol{\gamma}^{\Delta_1} = \underbrace{\begin{bmatrix}\mathbf{s}_1^{\Delta_1} & \mathbf{s}_2^{\Delta_1} & \mathbf{s}_3^{\Delta_1}\end{bmatrix}}_{\mathbf{s}^{\Delta_1}}\begin{bmatrix}\mathbf{d}_{eO}\\ \mathbf{d}_{e1}\\ \mathbf{d}_{e2}\end{bmatrix} = \mathbf{s}^{\Delta_1}\mathbf{d}^{\Delta_1} \qquad (28)$$

where $\mathbf{r}^{\Delta_1}$, $\mathbf{b}^{\Delta_1}$ and $\mathbf{s}^{\Delta_1}$ are, respectively, computed similarly

as the matrices $\mathbf{R}$, $\mathbf{B}$ and $\mathbf{S}$ of the DSG3 in Eqs. (13) and (16) but with two following changes: 1) the coordinates of three node $\mathbf{x}_i = \begin{bmatrix} x_i & y_i \end{bmatrix}^T, i = 1,2,3$ are replaced by $\mathbf{x}_O$, $\mathbf{x}_1$ and $\mathbf{x}_2$, respectively; and 2) the area $A_e$ is replaced by the area $A_{\Delta_1}$ of sub-triangle $\Delta_1$.

Substituting $\mathbf{d}_{eO}$ in Eq. (24) into Eqs. (26), (27) and (28), and then rearranging we obtain

$$\boldsymbol{\varepsilon}^{m\Delta_1} = \underbrace{\begin{bmatrix} \frac{1}{3}\mathbf{r}_1^{\Delta_1} + \mathbf{r}_2^{\Delta_1} & \frac{1}{3}\mathbf{r}_1^{\Delta_1} + \mathbf{r}_3^{\Delta_1} & \frac{1}{3}\mathbf{r}_1^{\Delta_1} \end{bmatrix}}_{\mathbf{R}^{\Delta_1}} \begin{bmatrix} \mathbf{d}_{e1} \\ \mathbf{d}_{e2} \\ \mathbf{d}_{e3} \end{bmatrix} = \mathbf{R}^{\Delta_1}\mathbf{d}_e \tag{29}$$

$$\boldsymbol{\kappa}^{\Delta_1} = \underbrace{\begin{bmatrix} \frac{1}{3}\mathbf{b}_1^{\Delta_1} + \mathbf{b}_2^{\Delta_1} & \frac{1}{3}\mathbf{b}_1^{\Delta_1} + \mathbf{b}_3^{\Delta_1} & \frac{1}{3}\mathbf{b}_1^{\Delta_1} \end{bmatrix}}_{\mathbf{B}^{\Delta_1}} \begin{bmatrix} \mathbf{d}_{e1} \\ \mathbf{d}_{e2} \\ \mathbf{d}_{e3} \end{bmatrix} = \mathbf{B}^{\Delta_1}\mathbf{d}_e \tag{30}$$

$$\boldsymbol{\gamma}^{\Delta_1} = \underbrace{\begin{bmatrix} \frac{1}{3}\mathbf{s}_1^{\Delta_1} + \mathbf{s}_2^{\Delta_1} & \frac{1}{3}\mathbf{s}_1^{\Delta_1} + \mathbf{s}_3^{\Delta_1} & \frac{1}{3}\mathbf{s}_1^{\Delta_1} \end{bmatrix}}_{\mathbf{S}^{\Delta_1}} \begin{bmatrix} \mathbf{d}_{e1} \\ \mathbf{d}_{e2} \\ \mathbf{d}_{e3} \end{bmatrix} = \mathbf{S}^{\Delta_1}\mathbf{d}_e \tag{31}$$

Similarly, by using cyclic permutation, we easily obtain the membrane strain $\boldsymbol{\varepsilon}^{m\Delta_2}$, $\boldsymbol{\varepsilon}^{m\Delta_3}$, the curvatures of the deflection $\boldsymbol{\kappa}^{\Delta_2}$, $\boldsymbol{\kappa}^{\Delta_3}$ and the altered shear strains $\boldsymbol{\gamma}^{\Delta_2}$, $\boldsymbol{\gamma}^{\Delta_3}$ for the second sub-triangle $\Delta_2$ and third sub-triangle $\Delta_3$, respectively.

Now, applying the cell-based strain smoothing operation in CS-FEM [12], the constant strains $\boldsymbol{\varepsilon}^{m\Delta_j}$, $\boldsymbol{\kappa}^{\Delta_j}$ and $\boldsymbol{\gamma}^{\Delta_j}$, $j = 1,2,3$, respectively, are used to create a smoothed membrane strain $\tilde{\boldsymbol{\varepsilon}}_e^m$, a smoothed bending strain $\tilde{\boldsymbol{\kappa}}_e$ and a smoothed shear strain $\tilde{\boldsymbol{\gamma}}_e$ on the element $\Omega_e$, such as:

$$\tilde{\boldsymbol{\varepsilon}}_e^m = \int_{\Omega_e} \boldsymbol{\varepsilon}^m \Phi_e(\mathbf{x})\,\mathrm{d}\Omega = \sum_{j=1}^{3} \boldsymbol{\varepsilon}^{m\Delta_j} \int_{\Delta_j} \Phi_e(\mathbf{x})\,\mathrm{d}\Omega \tag{32}$$

$$\tilde{\boldsymbol{\kappa}}_e = \int_{\Omega_e} \boldsymbol{\kappa}^h \Phi_e(\mathbf{x})\,\mathrm{d}\Omega = \sum_{j=1}^{3} \boldsymbol{\kappa}^{\Delta_j} \int_{\Delta_j} \Phi_e(\mathbf{x})\,\mathrm{d}\Omega \tag{33}$$

$$\tilde{\boldsymbol{\gamma}}_e = \int_{\Omega_e} \boldsymbol{\gamma}^h \Phi_e(\mathbf{x})\,d\Omega = \sum_{j=1}^{3} \boldsymbol{\gamma}^{\Delta_j} \int_{\Delta_j} \Phi_e(\mathbf{x})\,d\Omega \tag{34}$$

where $\Phi_e(\mathbf{x}) = \begin{cases} 1/A_e & \mathbf{x} \in \Omega_e \\ 0 & \mathbf{x} \notin \Omega_e \end{cases}$ is a constant smoothing function with $A_e$ is the area of the triangular element. The smoothed strains $\tilde{\boldsymbol{\varepsilon}}_e^m$, $\tilde{\boldsymbol{\kappa}}_e$ and $\tilde{\boldsymbol{\gamma}}_e$ in Eqs. (32), (33) and (34) now become

$$\tilde{\boldsymbol{\varepsilon}}_e^m = \tilde{\mathbf{R}}\mathbf{d}_e \;;\; \tilde{\boldsymbol{\kappa}}_e = \tilde{\mathbf{B}}\mathbf{d}_e \;;\; \tilde{\boldsymbol{\gamma}}_e = \tilde{\mathbf{S}}\mathbf{d}_e \tag{35}$$

where $\tilde{\mathbf{R}}$, $\tilde{\mathbf{B}}$, $\tilde{\mathbf{S}}$ are the smoothed strain gradient matrices, respectively, given by

$$\tilde{\mathbf{R}} = \frac{1}{A_e}\sum_{j=1}^{3} A_{\Delta_j}\mathbf{R}^{\Delta_j};$$
$$\tilde{\mathbf{B}} = \frac{1}{A_e}\sum_{j=1}^{3} A_{\Delta_j}\mathbf{B}^{\Delta_j};\; \tilde{\mathbf{S}} = \frac{1}{A_e}\sum_{j=1}^{3} A_{\Delta_j}\mathbf{S}^{\Delta_j} \tag{36}$$

Therefore the global stiffness matrix of the CS-DSG3 are assembled by

$$\tilde{\mathbf{K}} = \sum_{e=1}^{N_e} \tilde{\mathbf{K}}_e \tag{37}$$

where $\tilde{\boldsymbol{\kappa}}_e$ is the smoothed element stiffness given by

$$\begin{aligned} \tilde{\mathbf{K}}_e &= \mathbf{T}^T\left(\int_{\Omega_e} \tilde{\mathbf{R}}^T\mathbf{D}^m\tilde{\mathbf{R}}\,\mathrm{d}\Omega + \int_{\Omega_e} \tilde{\mathbf{B}}^T\mathbf{D}^b\tilde{\mathbf{B}}\,\mathrm{d}\Omega + \int_{\Omega_e} \tilde{\mathbf{S}}^T\mathbf{D}^s\tilde{\mathbf{S}}\,\mathrm{d}\Omega\right)\mathbf{T} \\ &= \mathbf{T}^T\underbrace{\left(\tilde{\mathbf{R}}^T\mathbf{D}^m\tilde{\mathbf{R}}\,A_e + \tilde{\mathbf{B}}^T\mathbf{D}^b\tilde{\mathbf{B}}\,A_e + \tilde{\mathbf{S}}^T\mathbf{D}^s\tilde{\mathbf{S}}\,A_e\right)}_{\tilde{\mathbf{k}}_e}\mathbf{T} = \mathbf{T}^T\tilde{\mathbf{k}}_e\mathbf{T} \end{aligned} \tag{38}$$

For free vibration analysis, we have

$$(\tilde{\mathbf{K}} - \omega^2\mathbf{M})\mathbf{d} = \mathbf{0} \tag{39}$$

where $\omega$ is the natural frequency and $\mathbf{M}$ is the global mass matrix defined by

$$\mathbf{M} = \int_{\Omega} \mathbf{N}^T\mathbf{m}\mathbf{N}^T\,\mathrm{d}\Omega \tag{40}$$

From Eq. (36) and (38), it is clearly seen that the element stiffness matrix in the CS-DSG3 does not depend on the sequence of node numbers, and hence the solution of CS-DSG3 is always stable when the sequence of node numbers changes.

## NUMERICAL RESULTS

In this section, two numerical examples are performed to show the accuracy and stability of the proposed CS-DSG3 compared to the analysis solutions. The stabilized parameter a in Eq. (23) in the CS-DSG3 is fixed at 0.1 for both static analysis and free vibration analysis. For comparison, several others flat shell elements such as DSG3 [9], DKT [16], MIN3 [17] and MITC4 [18] have also been implemented in our package. The membrane element used here in others triangular flat shell elements is the constant strain triangular element (CST), and hence three triangular flat shell elements used for comparion are abbreviated as DSG3-CST, DKT-CST and MIN3-CST.

### 4.1. Cylindrical Shell under Uniform Load - Scordelis-Lo roof

We now consider a cylindrical shell roof known as the Scordelis-Lo roof in which two curved edges are supported by rigid diaphragms *(u = w = 0)*, and the other two edges are free as shown in Figure 5. The Scordelis-Lo roof is subjected to the self-weight $q = 90$ per unit area in $z$ direction and has the geometric dimensions given by the length $L = 50$, the radius $R = 25$ and the thickness $t = 0.25$. The material properties are given by Poisson's ratio $v=0.0$ and Young's modulus $E = 4.32\times10^8$. This example was first modeled by Scordelis and Lo [19] who gave the mid-side vertical displacement at point A is 0.3086. However, many finite elements converge to a slightly smaller value, and hence Macneal and Harder [20] suggested to use the value of 0.3024 for testing. Due to its symmetry, only a quarter of the cylinder shell is modeled. Five uniform discretizations *NxN* of shell with $N$ = 4, 8, 10, 12 and 16 are used and two discretizations *16x16* using triangular and quadrilateral elements are plotted in Figure 6.

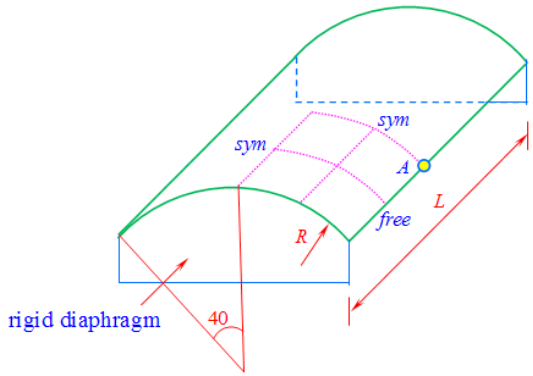


Figure 5: Geometry of the Scordelis-Lo roof in which two curved edges are supported by rigid diaphragms ($u = w = 0$), and the other two edges are free

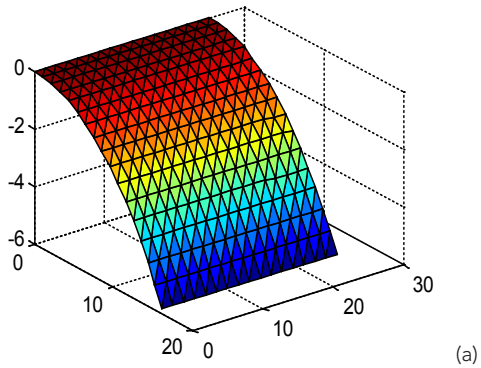


(a)

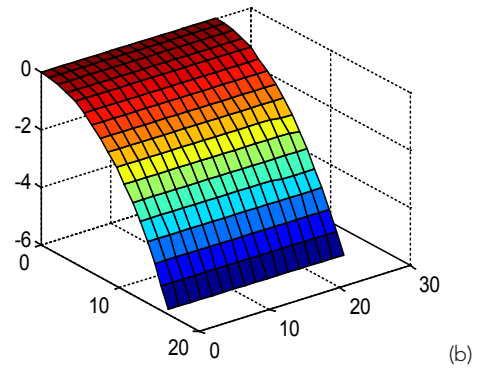


(b)

Figure 6: Two discretizations of a quarter of the Scordelis-Lo roof using (a) triangular elements; (b) quadrilateral elements

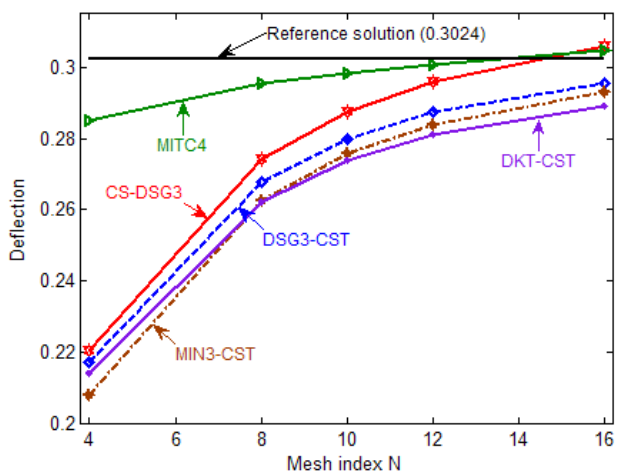


Figure 7: Convergence of mid-side vertical displacement at point A of Scordelis-Lo roof

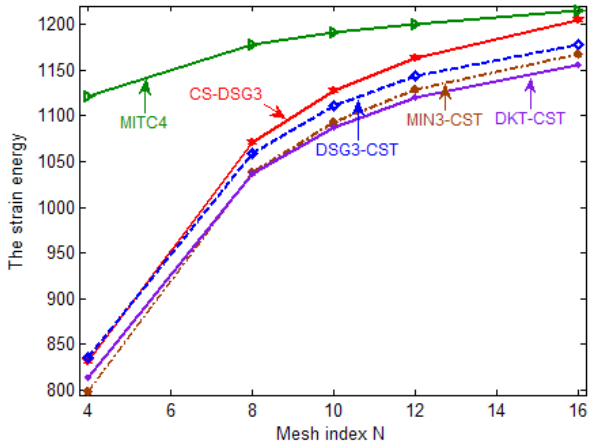


Figure 8: Convergence of the strain energy of the Scordelis-Lo roof

Figure 7 shows the convergence of the mid-side vertical displacement at point A obtained using structured meshes and different methods. It is seen that with the same degree of freedoms (DOFs), the results of the CS-DSG3 are better than those of almost methods and only worse than those of the MITC4 in some coarse meshes. Also note that, the CS-DSG3 shows the fastest convergence to the reference solution for the fine meshes.

Figure 8 shows the convergence of the strain energy obtained using structured meshes and different methods. The results again confirm the comments obtained the mid-side vertical displacement at point A shown in Figure 7.

### 4.2. Hemispherical Panel

Let us now consider a hemispherical panel as shown in Figure 9 with radius R = 1m, thickness t = 0.1m, $\varphi_0 = 30^\circ$, $\varphi_1 = 90^\circ$, $\psi = 120^\circ$. The material parameters are given by Youngs modulus $E$ =2.1×10$^{11}$ Pa, Poissons ratio $\nu$ = 0.3, mass density $\rho$ = 7800 kg/m$^3$. Four uniform discretizations $NxN$ of shell with $N$ = 8, 12, 16 and 20 are used and two discretizations 12x12 using triangular and quadrilateral elements are plotted in Figure 10.

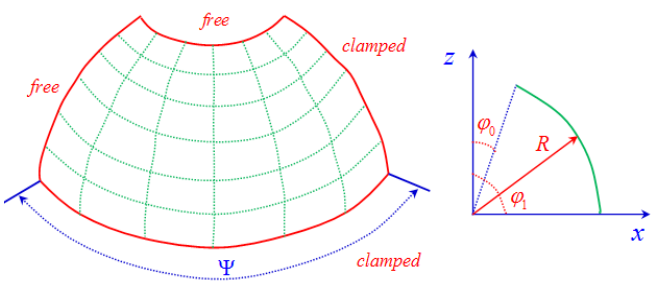


Figure 9: Geometry of the hemispherical panel with clamped at 2 edges and free at 2 edges

Eight lowest modes by the CS-DSG3 and various methods are plotted in Figure 11 with mesh 12x12. The results are also compared with the numerical solutions of the Generalized Differential Quadrature (GDQ) method [21] and the reference results derived from commercial software packages such as Abaqus, Ansys, Nastran, Straus found in Ref [21]. It is again observed that the results of CS-DSG3 converge well to the reference solutions of the GDQ [21] and of commercial software packages such as

Abaqus, Ansys, Nastran, Straus [21]. It is seen that CS-DSG3 is better than DSG3-CST, MIN3-CST, DKT-CST and a good competitor to the MITC4.

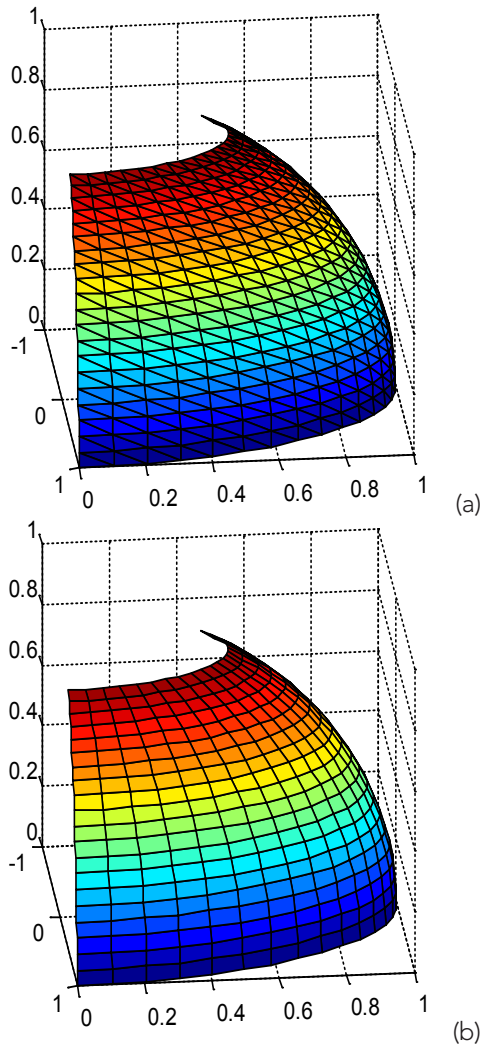


Figure 10: Two discretizations of hemispherical panel using (a) triangular elements; (b) quadrilateral elements

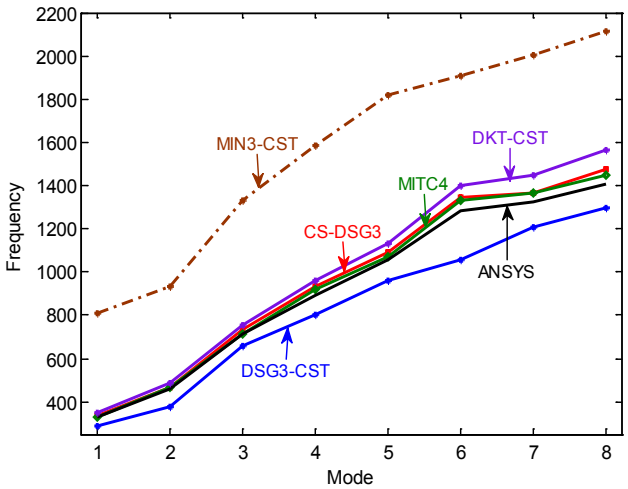


Figure 11: Eight lowest frequencies of hemispherical panel discretized by a mesh 12×12

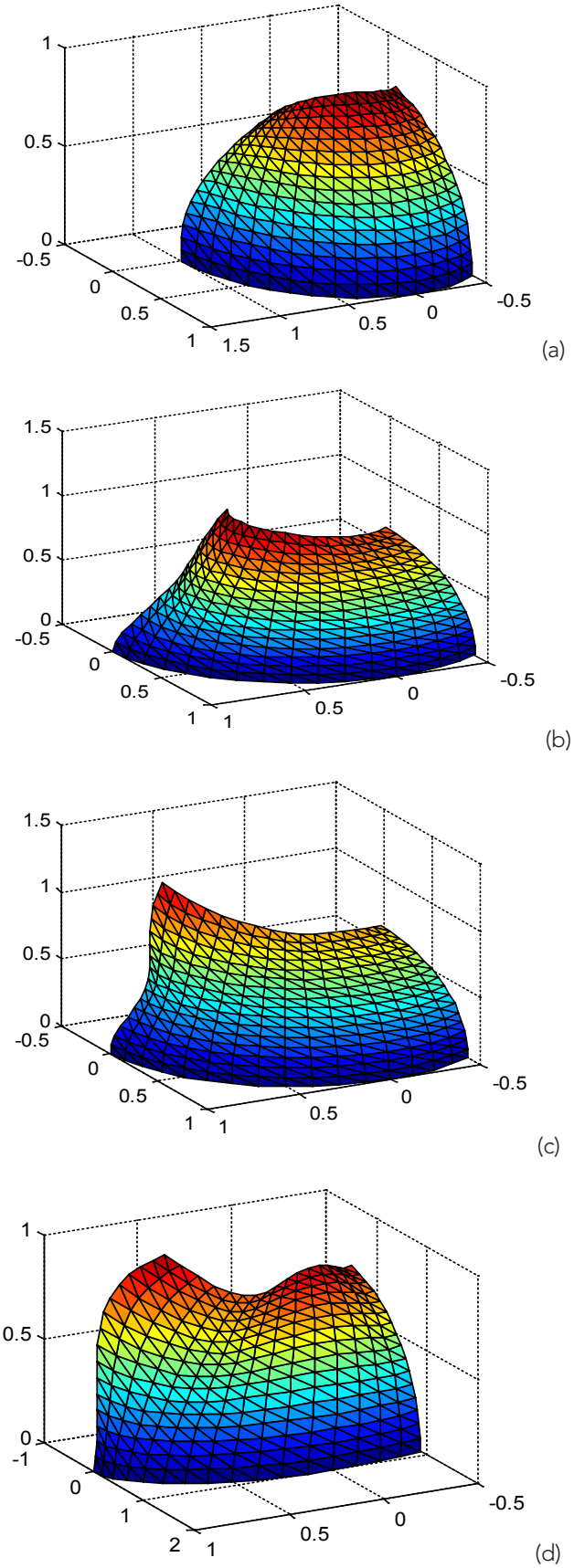


Figure 12: Shape of four lowest eigenmodes of the hemispherical panel with mesh 16×16 by the CS-DSG3. (a) Mode 1; (b) Mode 2; (c) Mode 3; (d) Mode 4

Figure 12 plots the shape of four lowest eigenmodes of the

hemispherical panel with mesh *16x16* by the CS-DSG3. It is seen that the shapes of eigenmodes express exactly the real physical modes of shell.

## CONCLUSIONS

A cell-based smoothed discrete shear gap method (CS-DSG3) for static and free vibration analyses of Reissner-Mindlin shells is formulated by combining the cell-based strain smoothing technique with the discrete shear gap method (DSG3) using three-node triangular elements. In the process of formulating the system stiffness matrix of the CS-DSG3, each triangular element will be divided into three sub-triangles, and in each sub-triangle, the stabilized DSG3 is used to compute the strains and to avoid the transverse shear locking. Then the strain smoothing technique on whole the triangular element is used to smooth the strains on these three sub-triangles. The CS-DSG3 hence not only overcomes the drawback of the DSG3 which depends on the sequence of node numbers of elements, but also improve the accuracy as well as the stability of the DSG3. The numerical examples demonstrated that the CS-DSG3 is free of shear locking and achieves the high accuracy compared to others existing flat shell elements.

Acknowledgements - This work was supported by Vietnam National Foundation for Science & Technology Development (NAFOSTED), Ministry of Science & Technology, under the basic research program (Project No.: 107.02.2010.01).

[1] Division of Computational Mechanics, Ton Duc Thang University,
98 Ngo Tat To St., Ward 19, Binh Thanh Dist., Hochiminh City, Vietnam
e-mail: thoitrung76@gmail.com, phucphungvan@gmail.com, thchien80@gmail.com, h.nguyenxuan@gmail.com, http://www.tut.edu.vn/

[2] Faculty of Mathematics & Computer Science, University of Science, Vietnam National University HCMC, 227 Nguyen Van Cu, Dist. 5, Hochiminh City, Vietnam
e-mail: ngttrung@hcmus.edu.vn, nxhung@hcmus.edu.vn, http://www.hcmus.edu.vn/

[3] Faculty of Civil Engineering, Ho Chi Minh City University of Technology (HCMUT),
268 Ly Thuong Kiet St, Dist 10, Hochiminh City, Vietnam
e-mail: lvhai@hcmut.edu.vn; http://www.ntt.edu.vn/

## REFERENCES

[1] J.N. Reddy. Theory and Analysis of Elastic Plates and Shells. CRC Press: Taylor and Francis Group, NewYork, 2006.
[2] T.Y. Henry Yang, S. Saigal, A. Masud, R.K. Kapania. A survey of recent shell finite elements. International Journal for Numerical Methods in Engineering 2000; 47: 101-127.
[3] T. Belytschko, I. Leviathan. Physical stabilization of the 4-node shell element with one-point quadrature. Computer Methods in Applied Mechanics and Engineering 1994; 113: 321-350.
[4] E.N. Dvorkin, K.J. Bathe. A continuum mechanics based four-node shell element for general non-linear analysis. Engineering Computations 1984; 1: 77-78.
[5] N. Carpenter, H. Stolarski, T. Belytschko. Improvements in 3-node triangular shell elements. International Journal for Numerical Methods in Engineering 1986; 23: 1643-1647.
[6] E. Onate, F. Zarate, F. Flores. A simple triangular element for thick and thin plate and shell analysis. International Journal for Numerical Methods in Engineering 1994; 37: 2569-2582.
[7] R.H. Macneal. Derivation of element stiffness matrices by assumed strain distributions. Nuclear Engineering and Design 1982; 70: 3-12.
[8] N. Nguyen-Thanh, Rabczuk Timon, H. Nguyen-Xuan, Bordas Stephane. A smoothed finite element method for shell analysis. Computer Methods in Applied Mechanics and Engineering 2008; 198: 165-177.
[9] K.U. Bletzinger, M. Bischoff, E. Ramm. A unified approach for shear-locking free triangular and rectangular shell finite elements. Computers and Structures 2000; 75: 321-334.
[10] G.R. Liu, Nguyen Thoi Trung. Smoothed Finite Element Methods. CRC Press, Taylor and Francis Group, NewYork, 2010.
[11] G.R. Liu, K.Y. Dai, T. Nguyen-Thoi. A smoothed finite element for mechanics problems. Computational Mechanics 2007; 39: 859-877.
[12 G.R. Liu, T. Nguyen-Thoi, K.Y. Dai, K.Y. Lam. Theoretical aspects of the smoothed finite element method (SFEM). International Journal for Numerical Methods in Engineering 2007; 71: 902-930.
[13 J.S. Chen, C.T. Wu, S. Yoon, Y. You. A stabilized conforming nodal integration for galerkin mesh-free methods. International Journal for Numerical Methods in Engineering 2001; 50: 435-466.
[14] M. Bischoff, K.U. Bletzinger. Stabilized DSG plate and shell elements. Trends in computational structural mechanics, CIMNE, Barcelona, Spain 2001.
[15] M. Lyly, R. Stenberg, T. Vihinen. A stable bilinear element for the Reissner–Mindlin plate model. Computer Methods Applied Mechanics Engineering 1993; 110: 343-357.
[16] J.L. Batoz, K.J. Bathe, L.W. Ho. A study of three-node triangular plate bending elements. International Journal for Numerical Methods in Engineering 1980; 15: 1771-1812.
[17] A. Tessler, T.J.R. Hughes. A three-node mindlin plate element with improved transverse shear. Computer Methods Applied Mechanics Engineering 1985; 50: 71-101.
[18] K.J. Bathe, E.N. Dvorkin. A four-node plate bending element based on Mindlin–Reissner plate theory and a mixed interpolation. International Journal for Numerical Methods in Engineering 1985; 21: 367-383.
[19] A.C. Scordelis, K.S. Lo. Computer analysis of cylindrical shells. J. Amer. Concrete Inst 1964; 61:539-561.
[20] R.H. McNeal, R.L. Harder. A proposed set of problems to test finite element accuracy. Finite Elem. Anal. 1985; 1: 3-20.
[21] T. Francesco, V. Erasmo. Vibration analysis of spherical structural elements using the GDQ method. Computers and Mathematics with Applications 2007; 53: 1538-1560.